Accelerated Optimality-based Bound Tightening Algorithm for Interval State Estimation of Low Voltage Networks

Suntao Su, Liang Du
Dept. of Electrical and Computer Engineering
Villanova University
Villanova, PA, USA
ssu02@villanova.edu, liang.du@villanova.edu

Junbo Zhao
Thayer School of Engineering
Dartmouth College
Hanover, NH, USA
junbo.zhao@dartmouth.edu

***Abstract*—The presence of uncertainties of measurement errors and residential solar generation complicates state estimation of low voltage (LV) networks. To address that, an interval state estimation (ISE) approach for LV networks is proposed in this work. A linear relaxation-based ISE model is first developed by incorporating McCormick envelopes into the three-phase unbalanced non-convex ISE formulation, allowing efficient computation, while ensuring near-global optimality. Subsequently, the polar form of state variables is reconstructed using the feasible solution obtained from the relaxed ISE model. To improve efficiency, an accelerated optimality-based bound tightening algorithm is proposed to derive tight variable bounds, integrating three accelerated strategies: variable ordering, bound filtering, and asynchronous bound tightening. Numerical results verify that compared to existing methods, the proposed ISE method reduces computational effort without losing the estimation accuracy.**

***Index Terms*—Interval state estimation, McCormick envelopes, Accelerated OBBT algorithm, Low voltage networks.**

I. Introduction

The growing integration of distributed generators (DGs), such as residential photovoltaic (PV) systems, has introduced significant uncertainty into low-voltage (LV) distribution networks. Unlike medium-voltage (MV) systems, LV networks are characterized by limited measurement infrastructure—typically only smart meters—along with inaccurate phase connectivity information and highly stochastic, localized power injections from household-level DGs [1]. These factors make LV networks inherently more complex to monitor and control. Consequently, near real-time monitoring has become increasingly critical to support and maintain power quality.

State estimation (SE) is a fundamental process in power and distribution systems for real-time monitoring and control. However, achieving observability in LV networks often depends on pseudo-measurements, which tend to be less accurate than real sensor data. Furthermore, due to numerous sources of uncertainty in the measurement process, the exact probability distribution of measurement errors is often unknown in practice [2]. As a result, traditional weighted least squares (WLS) methods [3], which rely on assumed statistical models of measurement noise, struggle to capture the full extent of uncertainty in both data and models.

To address these challenges, interval SE (ISE) has emerged as a promising alternative. Rather than treating measurements and parameters as fixed values, ISE represents them as intervals that encapsulate uncertainty, yielding upper and lower bounds on system states. Early work applied interval arithmetic to directly solve ISE problems, as in the WLS-based ISE framework for MV networks solved using a modified Krawczyk operator (KO) [4]. However, interval arithmetic methods often produce conservative estimates due to the wrapping effect. Interval constraint propagation (ICP) techniques [5] have been explored as an alternative, but they can over-relax constraints by neglecting correlations among variables. More recently, approaches based on relative distance measure arithmetic [6] have been proposed to mitigate conservativeness and tighten estimation bounds.

Another line of research formulates ISE as an optimization problem [7], which can yield narrower interval estimates. For instance, the method in [8] defines the ISE as an optimization model with inequality constraints representing measurement uncertainty bounds for LV networks. Although effective, this model is nonconvex and typically solved using interior-point methods, which cannot guarantee global optimality.

To handle such nonconvexity, several relaxation techniques, such as McCormick relaxations, semidefinite programming (SDP), second-order cone (SOC) programming, and quadratic convex (QC) relaxations, have been widely used in power system optimization [9]. In particular, the optimality-based bound tightening (OBBT) algorithm [10] can significantly narrow variable bounds by iteratively solving relaxed models. However, OBBT is computationally intensive, as it requires solving up to twice the number of linear programs (LPs) as there are variables in each iteration [11].

The objective of this work is to propose a computationally efficient framework that reformulates the nonconvex ISE model as a convex LP model using McCormick envelopes. To further accelerate computation, an accelerated OBBT (AOBBT) algorithm is developed, reducing the cost of bound tightening while maintaining solution accuracy. By integrating McCormick relaxations with AOBBT, the proposed approach

979-8-3315-8138-1

produces tighter feasible regions for LV network measurement equations under uncertainty and achieves convergence to near-optimal state bounds efficiently.

II. Nonlinear Programming-based ISE Model for LV Networks

State variables are selected as the real and imaginary parts of voltages for three phases at non-slack buses. The measurement equations of a three-phase LV network can be written as

$$\boldsymbol{z} = \boldsymbol{h}(\boldsymbol{x}) + \boldsymbol{w} \tag{1}$$

where $\boldsymbol{z}$ is the vector of measurements; $\boldsymbol{w}$ is the vector of measurement errors; $\boldsymbol{h}(\boldsymbol{x})$ is the vector of nonlinear three-phase measurement equations.

The 3σ rule of the Gaussian distribution is used to determine bounds of measurement errors, i,e,. $-3\sigma \leq \omega \leq 3\sigma$. The upper and lower bounds of PV outputs can be predicted using the historical statistics of the PV outputs and their corresponding meteorological data. Thus, the uncertain PV outputs can be defined as $\underline{z}_{\text{PV}} \leq z_{\text{PV}} \leq \overline{z}_{\text{PV}}$. The optimization-based method is used to estimate the entire interval range for the state variables, accounting for the uncertainty. By minimizing and maximizing each state variable of interest subject to all the measurement inequality constraints, the method derives the lower and upper bounds of state variables. The ISE problem for LV networks can thus be formulated as a non-convex nonlinear program (NP), as follows:

$$\begin{aligned} &\min_{\boldsymbol{x}}(\max) \quad \boldsymbol{a}_t^{\mathrm{T}}\boldsymbol{x},\ t = 1, 2, ..., 2n \\ &\text{s.t.} \quad \begin{cases} \underline{z}_{P_i^\varphi} \leq h_{P_i^\varphi}(\boldsymbol{x}) \leq \overline{z}_{P_i^\varphi},\ i \in \mathcal{N}_P \\ \underline{z}_{Q_i^\varphi} \leq h_{Q_i^\varphi}(\boldsymbol{x}) \leq \overline{z}_{Q_i^\varphi},\ i \in \mathcal{N}_Q \\ \underline{z}_{P_{ij}^\varphi} \leq h_{P_{ij}^\varphi}(\boldsymbol{x}) \leq \overline{z}_{P_{ij}^\varphi},\ (i,j) \in \mathcal{L}_P \\ \underline{z}_{Q_{ij}^\varphi} \leq h_{Q_{ij}^\varphi}(\boldsymbol{x}) \leq \overline{z}_{Q_{ij}^\varphi},\ (i,j) \in \mathcal{L}_Q \\ \underline{z}_{V_i^\varphi} \leq h_{V_i^\varphi}(\boldsymbol{x}) \leq \overline{z}_{V_i^\varphi},\ i \in \mathcal{B} \end{cases} \end{aligned} \tag{2}$$

where n is the number of nodes; $\boldsymbol{a}_t \in \mathbb{R}^{2n\times 1}$ is the unit vector with its t-th element equal to 1, while all other elements are zero; $z_{P_i^\varphi}$ and $z_{Q_i^\varphi}$ are active and reactive power injection measurements of phase $\varphi \in \{a, b, c\}$ at bus i, respectively; $z_{P_{ij}^\varphi}$ and $z_{Q_{ij}^\varphi}$ are active and reactive power flow measurements of phase φ from bus i to bus j, respectively; $z_{V_i^\varphi}$ is the voltage magnitude measurement of phase φ at bus i; $\mathcal{N}_P, \mathcal{N}_Q, \mathcal{L}_P, \mathcal{L}_Q, \mathcal{B}$ are sets of corresponding measurements.

III. Proposed Linear Relaxation-based ISE Model for LV Networks

A. Stage I: Optimal Interval Solution

The non-convex model is first reformulated into a convex one using the linear relaxation technique. The only non-convex components in the ISE model for LV networks are the bilinear terms, which originate from $\boldsymbol{h}(\boldsymbol{x})$. These terms, which include $e_i^\varphi e_j^\psi,\ e_i^\varphi f_j^\psi,\ f_i^\varphi f_j^\psi,\ f_i^\varphi e_j^\psi,\ e_i^\varphi e_i^\varphi,\ f_i^\varphi f_i^\varphi$, can be redefined using six types of augmented variables, as follows:

$$\begin{cases} X_l^{\varphi\psi} = e_i^\varphi e_j^\psi,\ M_l^{\varphi\psi} = e_i^\varphi f_j^\psi,\ Y_l^{\varphi\psi} = f_i^\varphi f_j^\psi \\ N_l^{\varphi\psi} = f_i^\varphi e_j^\psi,\ R_i^{\varphi\varphi} = e_i^\varphi e_i^\varphi,\ K_i^{\varphi\varphi} = f_i^\varphi f_i^\varphi \end{cases} \tag{3}$$

By applying McCormick envelopes, these equality constraints are replaced with linear inequality constraints. Consequently, the non-convex ISE model is reformulated into a linear relaxation-based ISE model, as follows:

$$\min_{\{\boldsymbol{x},\boldsymbol{X},\boldsymbol{M},\boldsymbol{Y},\boldsymbol{N},\boldsymbol{R},\boldsymbol{K}\}}(\max) \quad \boldsymbol{a}_t^{\mathrm{T}}\boldsymbol{x},\ t = 1, 2, ..., 2n \tag{4}$$

$$\text{s.t.} \quad \underline{z}_{P_i^\varphi} \leq \boldsymbol{H}_{P_i^\varphi}\boldsymbol{B} \leq \overline{z}_{P_i^\varphi},\ i \in \mathcal{N}_P \tag{5}$$

$$\underline{z}_{Q_i^\varphi} \leq \boldsymbol{H}_{Q_i^\varphi}\boldsymbol{B} \leq \overline{z}_{Q_i^\varphi},\ i \in \mathcal{N}_Q \tag{6}$$

$$\underline{z}_{P_{ij}^\varphi} \leq \boldsymbol{H}_{P_{ij}^\varphi}\boldsymbol{B} \leq \overline{z}_{P_{ij}^\varphi},\ (i,j) \in \mathcal{L}_P \tag{7}$$

$$\underline{z}_{Q_{ij}^\varphi} \leq \boldsymbol{H}_{Q_{ij}^\varphi}\boldsymbol{B} \leq \overline{z}_{Q_{ij}^\varphi},\ (i,j) \in \mathcal{L}_Q \tag{8}$$

$$\underline{z}^2_{V_i^\varphi} \leq \boldsymbol{H}_{V_i^\varphi}\boldsymbol{B} \leq \overline{z}^2_{V_i^\varphi},\ i \in \mathcal{B} \tag{9}$$

$${X_l}^{\varphi\psi} - \underline{e_i^\varphi}e_j^\psi - \underline{e_j^\psi}e_i^\varphi + \underline{e_i^\varphi}\,\underline{e_j^\psi} \geq 0,\ l \in \mathcal{L} \tag{10}$$

$${X_l}^{\varphi\psi} - \overline{e_i^\varphi}e_j^\psi - \overline{e_j^\psi}e_i^\varphi + \overline{e_i^\varphi}\,\overline{e_j^\psi} \geq 0,\ l \in \mathcal{L} \tag{11}$$

$${X_l}^{\varphi\psi} - \underline{e_i^\varphi}e_j^\psi - \overline{e_j^\psi}e_i^\varphi + \underline{e_i^\varphi}\,\overline{e_j^\psi} \leq 0,\ l \in \mathcal{L} \tag{12}$$

$${X_l}^{\varphi\psi} - \overline{e_i^\varphi}e_j^\psi - \underline{e_j^\psi}e_i^\varphi + \overline{e_i^\varphi}\,\underline{e_j^\psi} \leq 0,\ l \in \mathcal{L} \tag{13}$$

$$\cdots \tag{14}$$

$$\underline{e_i^\varphi} \leq e_i^\varphi \leq \overline{e_i^\varphi},\ \underline{f_i^\varphi} \leq f_i^\varphi \leq \overline{f_i^\varphi},\ i \in \mathcal{B} \tag{15}$$

$$\underline{e_i^\psi} \leq e_i^\psi \leq \overline{e_i^\psi},\ \underline{f_i^\psi} \leq f_i^\psi \leq \overline{f_i^\psi},\ i \in \mathcal{B} \tag{16}$$

where $\mathcal{L}$ is the set of all real branches; Envelopes of augmented variables $\{\boldsymbol{M}, \boldsymbol{Y}, \boldsymbol{N}, \boldsymbol{R}, \boldsymbol{K}\}$ which are omitted in Eq.(14) for brevity, are similar to Eqs. (10)-(13). See [12] for details.

For the sake of brevity, the above linear relaxation-based ISE model for LV networks can be condensed as follows:

$$\begin{aligned} &\min_{\{\boldsymbol{x},\boldsymbol{B}\}}(\max) \quad \boldsymbol{a}_t^{\mathrm{T}}\boldsymbol{x},\ t = 1, 2, ..., 2n \\ &\text{s.t.} \quad \begin{cases} \underline{\boldsymbol{z}} \leq \boldsymbol{H}\boldsymbol{B} \leq \overline{\boldsymbol{z}} \\ \text{Eqs. (10)-(16)} \end{cases} \end{aligned} \tag{17}$$

where $\boldsymbol{B} = [\boldsymbol{X}^{\mathrm{T}}\ \boldsymbol{M}^{\mathrm{T}}\ \boldsymbol{Y}^{\mathrm{T}}\ \boldsymbol{N}^{\mathrm{T}}\ \boldsymbol{R}^{\mathrm{T}}\ \boldsymbol{K}^{\mathrm{T}}]^{\mathrm{T}}$ is the vector of all bilinear terms and $\boldsymbol{H}$ represents the linear function.

B. Stage II: State Reconstruction

Eq. (17) formulates the upper and lower bounds of the real and imaginary parts of voltages. However, voltage magnitudes and phase angles are more convenient for operators to understand the operating state of the system. The polar form of state variables can be derived by modifying the model's objective function and introducing additional constraints. Let LR_Ω represent the constraints defined in Eq. (17).

1) *Voltage Magnitude*: The voltage magnitude intervals can be obtained by solving the original problem with a replaced objective function $V_i^\varphi = \sqrt{R_i^{\varphi\varphi} + K_i^{\varphi\varphi}} = \sqrt{H_{V_i^\varphi}}$. Due to the nonlinearity introduced by the square root, Eq. (18) is first solved to determine the square voltage magnitudes. Subsequently, the interval for the voltage magnitude is calculated using square root arithmetic. For $i \in \mathcal{B}$:

$$\begin{cases} (\underline{V}_i^\varphi)^2 \Leftarrow \{\min H_{V_i^\varphi}\boldsymbol{B} \quad \text{s.t. } LR_\Omega \cap \Omega_x\} \\ (\overline{V}_i^\varphi)^2 \Leftarrow \{\min -H_{V_i^\varphi}\boldsymbol{B} \quad \text{s.t. } LR_\Omega \cap \Omega_x\} \end{cases} \tag{18}$$

2) *Voltage Phase Angle*: The voltage phase angle intervals can be obtained by solving the original problem with the replaced objective function $\theta_i^{\varphi} = \arctan(f_i^{\varphi}/e_i^{\varphi})$. To accurately determine the voltage angle within the range $[-2\pi, 2\pi]$ and account for the correct quadrant, θ_i^{φ} is expressed as a piecewise function that considers the signs of f_i^{φ} and e_i^{φ}, as follows:

$$\theta_i^{\varphi} = \begin{cases} \arctan(f_i^{\varphi}/e_i^{\varphi}), & e_i^{\varphi} > 0 \\ \arctan(f_i^{\varphi}/e_i^{\varphi}) + \pi, & f_i^{\varphi} \geq 0, e_i^{\varphi} < 0 \\ \arctan(f_i^{\varphi}/e_i^{\varphi}) - \pi, & f_i^{\varphi} < 0, e_i^{\varphi} < 0 \\ \pi/2, & e_i^{\varphi} = 0 \text{ and } f_i^{\varphi} > 0 \\ -\pi/2, & e_i^{\varphi} = 0 \text{ and } f_i^{\varphi} < 0 \end{cases} \tag{19}$$

A dummy vector $\boldsymbol{y}$, where $y_i^{\varphi} = f_i^{\varphi}/e_i^{\varphi}$, can be reformulated as the bilinear term $f_i^{\varphi} = y_i^{\varphi} e_i^{\varphi}$. McCormick relaxation is then applied to generate envelopes, as follows:

$$f_i^{\varphi} - \underline{e_i^{\varphi}} y_i^{\varphi} - \underline{y_i^{\varphi}} e_i^{\varphi} + \underline{e_i^{\varphi}}\,\underline{y_i^{\varphi}} \geq 0,\ i \in \mathcal{B} \tag{20}$$
$$f_i^{\varphi} - \overline{e_i^{\varphi}} y_i^{\varphi} - \overline{y_i^{\varphi}} e_i^{\varphi} + \overline{e_i^{\varphi}}\,\overline{y_i^{\varphi}} \geq 0,\ i \in \mathcal{B} \tag{21}$$
$$f_i^{\varphi} - \underline{e_i^{\varphi}} y_i^{\varphi} - \overline{y_i^{\varphi}} e_i^{\varphi} + \underline{e_i^{\varphi}}\,\overline{y_i^{\varphi}} \leq 0,\ i \in \mathcal{B} \tag{22}$$
$$f_i^{\varphi} - \overline{e_i^{\varphi}} y_i^{\varphi} - \underline{y_i^{\varphi}} e_i^{\varphi} + \overline{e_i^{\varphi}}\,\underline{y_i^{\varphi}} \leq 0,\ i \in \mathcal{B} \tag{23}$$

Therefore, the upper and lower bound of y_i^{φ} can be obtained by solving the following linear program. For $i \in \mathcal{B}$:

$$\begin{cases} \underline{y_i^{\varphi}} \Leftarrow \{\min y_i^{\varphi} \quad \text{s.t. } LR_{\Omega*} \cap \Omega_x\} \\ \overline{y_i^{\varphi}} \Leftarrow \{\min -y_i^{\varphi} \quad \text{s.t. } LR_{\Omega*} \cap \Omega_x\} \end{cases} \tag{24}$$

where the $LR_{\Omega*}$ represents the constraints in Eq. (17) and Eqs. (20)-(23).

IV. Solution Methodology

A. Optimality-based Bound Tightening Algorithm

To determine the tightest possible state intervals, the OBBT algorithm is used to solve the linear relaxation-based ISE model for LV networks. The framework of the OBBT algorithm is outlined in Algorithm 1. The initial interval vector of variables is obtained by applying a conservative bound $[\underline{\boldsymbol{x}}^0, \overline{\boldsymbol{x}}^0]$. In Step 1, perform bounding linearization for all bilinear terms. In Step 2, the LPs shown in Eq. (17) are solved using any state-of-the-art solver. In Step 3, the estimated state intervals are updated by calculating the intersection of the newly obtained and previous intervals. In Step 4, the algorithm stops if the termination criterion is satisfied; otherwise, it returns to Step 1.

Algorithm 1 OBBT.

Initialization: Tolerance $\varepsilon,\ k=1,\ [\underline{\boldsymbol{x}}^0,\ \overline{\boldsymbol{x}}^0]$
Repeat:
Step 1. *Linear Relaxation*: Perform bounding linearization of bilinear terms using the bound $[\underline{\boldsymbol{x}}^{k-1}, \overline{\boldsymbol{x}}^{k-1}]$.
Step 2. *Bound Tightening*: Solve the LP problems in Eq. (17), and obtain the bound $[\underline{\boldsymbol{x}}^k, \overline{\boldsymbol{x}}^k]$.
Step 3. *Intersection*: Update the solution hull by tanking the intersection of intervals

$$\Omega_x^k \leftarrow [\underline{\boldsymbol{x}}^k, \overline{\boldsymbol{x}}^k] = [\underline{\boldsymbol{x}}^k, \overline{\boldsymbol{x}}^k] \cap [\underline{\boldsymbol{x}}^{k-1}, \overline{\boldsymbol{x}}^{k-1}].$$

Step 4. *Termination Criterion*: Stop if

$$\|\underline{\boldsymbol{x}}^k - \underline{\boldsymbol{x}}^{k-1}\|_\infty \leq \varepsilon \text{ and } \|\ \overline{\boldsymbol{x}}^k - \overline{\boldsymbol{x}}^{k-1}\ \|_\infty \leq \varepsilon;$$

Otherwise, $k \leftarrow k+1$ and return to Step 1.

B. Accelerated Optimality-based Bound Tightening Algorithm

The classical OBBT algorithm computes the tightest bounds of all state variables by minimizing and maximizing each variable within the relaxation framework. However, a full OBBT iteration requires solving $4n$ LPs, which makes it computationally expensive for large-scale systems. To improve efficiency, three acceleration strategies are integrated into the classical OBBT algorithm: variable ordering, bound filtering, and asynchronous bound tightening. The overall framework of the proposed AOBBT algorithm is presented in Algorithm 2.

1) Variable Ordering: An effective variable ordering strategy not only reduces the total number of LP iterations but also ensures the reliability of the tightened bounds. In LV networks, the reference bus on the primary side of the distribution transformer typically has fixed states. Nodes closer to this reference bus generally require fewer iterations for bound tightening and should therefore be prioritized. Conversely, variables associated with nodes farther from the reference bus, where residential PV systems are often connected and uncertainties are higher, offer a higher potential for tightening and should be explored later in the process.

2) Bound Filtering: The bound filtering strategy avoids redundant computations by skipping variables whose bounds no longer change significantly. Specifically, for a optimal solution $\tilde{x}_i \in LR_{\Omega}$, if its current solution satisfies $|\tilde{x}_i - l_i| \leq \delta$ or $|\tilde{x}_i - u_i| \leq \delta$. where $[l_i, u_i]$ represents the variable's current bound and δ is a small threshold fraction of the domain size, the corresponding bound is considered filtered and remains fixed in subsequent iterations. This selective filtering effectively reduces the total number of LPs solved from the original $4n$, reducing computational effort.

3) Asynchronous Bound Tightening: In the classical OBBT algorithm, synchronous bound tightening is employed, where bounds remain fixed throughout each iteration. Although this strategy is order-independent and easier to analyze theoretically, it limits performance since LPs cannot benefit from updated bounds until the next iteration.

To overcome this limitation, the proposed asynchronous bound tightening strategy introduces a step size parameter s, defined as the maximum number of LPs solved in pareller per micro-round. After solving s LPs, their corresponding bounds are immediately updated in the global variable box. Subsequent LPs in the same iteration can thus utilize these tightened bounds, allowing faster propagation and earlier convergence. Although results may depend on the order of variable processing, this approach typically achieves faster convergence without compromising accuracy.

Algorithm 2 AOBBT.

Initialization: Tolerance δ and ε, $K=1$, step size s, bound indices $\mathscr{L}, \mathscr{U} \in \{1,...,2n\}$, $[\underline{\boldsymbol{x}}^0,\ \overline{\boldsymbol{x}}^0]$

Repeat:

Step 1. *Linear Relaxation*: Perform bounding linearization of bilinear terms using the bound $[\underline{\boldsymbol{x}}^{K-1}, \overline{\boldsymbol{x}}^{K-1}]$.

Step 2. *Variable Ordering*: Build order val by physical distance from each node to the reference bus.

Step 3. *Asynchronous Bound Tightening*: Following the order val, solve s LPs in parallel to obtain the updated bounds $[\underline{\boldsymbol{x}}^K, \overline{\boldsymbol{x}}^K]$. Then refine the solution hull by taking the intersection of the intervals:

$$\Omega_x^K \leftarrow [\underline{\boldsymbol{x}}^K, \overline{\boldsymbol{x}}^K] = [\underline{\boldsymbol{x}}^K, \overline{\boldsymbol{x}}^K] \cap [\underline{\boldsymbol{x}}^{K-1}, \overline{\boldsymbol{x}}^{K-1}].$$

Repeat this process until all elements in val have been processed.

Step 4. *Bound Filtering*: Compute a feasible relaxation solution $\tilde{x}^K \in LR_\Omega$. Remove the k_lth lower bound, i,e., $\mathscr{L} \leftarrow \mathscr{L} \backslash k_l$ if

$$|\tilde{x}_{k_l}^K - \underline{x}_{k_l}^K| \leq \delta \text{ and } |\underline{x}_{k_l}^K - \underline{x}_{k_l}^{K-1}| \leq \varepsilon;$$

Remove the k_uth upper bound, i,e., $\mathscr{U} \leftarrow \mathscr{U} \backslash k_u$ if

$$|\tilde{x}_{k_u}^K - \overline{x}_{k_u}^K| \leq \delta \text{ and } |\overline{x}_{k_u}^K - \overline{x}_{k_u}^{K-1}| \leq \varepsilon.$$

Step 5. *Termination Criterion*: Stop if $\mathscr{L} \cup \mathscr{U} = \emptyset$; or

$$\|\underline{\boldsymbol{x}}^k - \underline{\boldsymbol{x}}^{k-1}\|_\infty \leq \varepsilon \text{ and } \|\ \overline{\boldsymbol{x}}^k - \overline{\boldsymbol{x}}^{k-1}\ \|_\infty \leq \varepsilon,$$

Otherwise, $K = K+1$, $s = s+16$ and return to Step 1.

V. Numerical Results

Two unbalanced LV feeders of different scales are used for testing. Their topology and parameters can be found in [13]. Residential PV systems are assumed to operate at unity power factor without any control functionalities. The available measurements include active and reactive power injections, voltage magnitudes, and active and reactive power flows at the start side of branches. It is assumed that all buses are equipped with smart meters. For unmeasured quantities, such as branch power flows, pseudo-measurements are generated and modeled with slightly higher errors than those of real measurements. All simulations are performed on a workstation equipped with an Intel Core i9 processor and 128 GB of RAM.

A. Estimation Performance

This section evaluates the performance of the proposed ISE method on a 121-node LV network. The proposed method is compared with two existing approaches: the NP-based ISE introduced in [8] and the KO-based ISE method described in [4]. The results from a Monte Carlo simulation (MCS)-based deterministic SE approach are used as the benchmark. Two performance metrics are employed to assess estimation quality. Average Interval Width (AIW) aims to quantify the mean width of the estimated state intervals, reflecting estimation tightness. Maximum Absolute Deviation (MAD) aims to measure the largest deviation between the estimated intervals and the true values, indicating the worst-case estimation error. The mathematical definitions of them are expressed as follows:

$$\text{AIW} = (1/n) \sum_{i=1}^{n} (\bar{x}_i - \underline{x}_i) \tag{25}$$

$$\text{MAD} = \max\left(|\bar{\boldsymbol{x}} - \bar{\boldsymbol{x}}^*|, |\underline{\boldsymbol{x}} - \underline{\boldsymbol{x}}^*|\right) \tag{26}$$

where $\overline{x}_i$ represents the i-th element of the upper bound vector $\overline{\boldsymbol{x}}$, $\underline{x}_i$ is the i-th element of the lower bound vector $\underline{\boldsymbol{x}}$; $\bar{\boldsymbol{x}}^*$ and $\underline{\boldsymbol{x}}^*$ denotes the upper and lower bounds of the true interval vectors derived from MCS method, respectively.

The estimation accuracy of different ISE methods is summarized in Table I. As shown, the proposed method achieves AIW and MAD values that are much closer to those of the MCS benchmark than those obtained using the NP and KO methods. Furthermore, when integrated with the AOBBT algorithm, the proposed method maintains comparable estimation accuracy to that achieved with the classical OBBT algorithm.

TABLE I
THE ESTIMATION ACCURACY ($\times 10^{-4}$ FOR AIW AND MAD VALUES)

Methods	V_m^{AIW}	V_a^{AIW}	V_m^{MAD}	V_a^{MAD}
KO	6.643	5.433	7.564	4.873
NP	3.587	3.085	4.355	2.715
MCS	1.327	1.067	\	\
Proposed (OBBT)	1.819	1.244	2.020	1.218
Proposed (AOBBT, s=16)	1.521	1.196	1.596	1.049
Proposed (AOBBT, s=64)	1.819	1.461	1.855	0.966
Proposed (AOBBT, s=128)	1.856	1.608	1.955	1.501
Proposed (AOBBT, s=256)	2.016	1.696	1.798	1.473

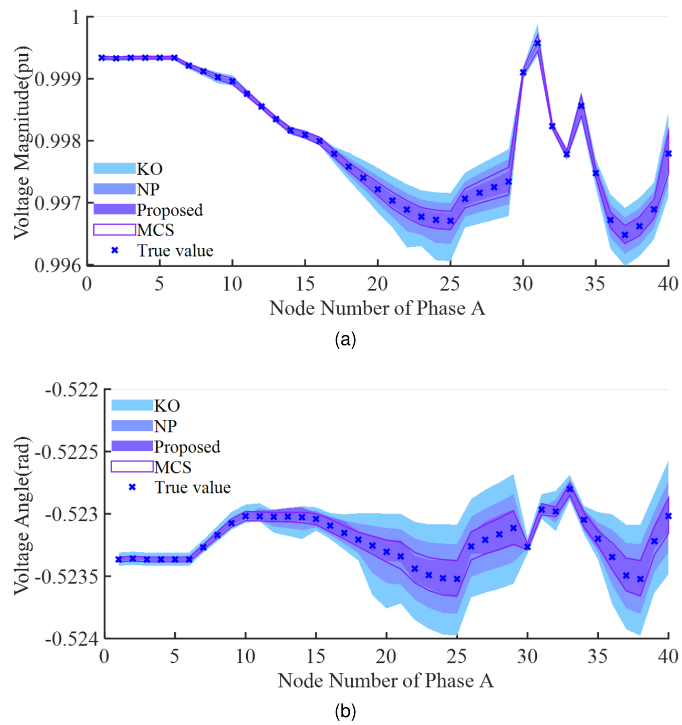

Fig. 1. Comparison of estimated intervals of different methods of phase A.

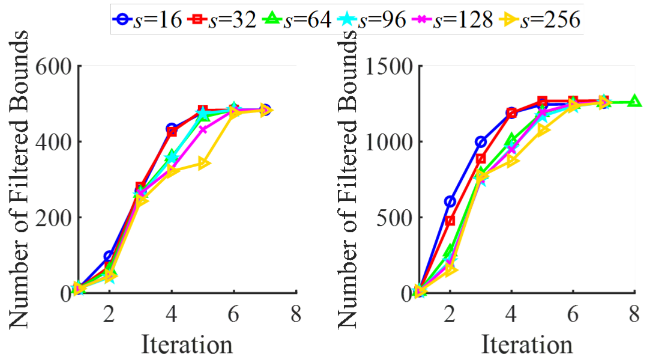

Fig. 2. The number of filtered bounds in the process of convergence for 121-node (left) and 321-node (right) LV network.

To provide a more intuitive comparison, Fig. 1 illustrates the estimated interval bounds of phase A under different methods, with a measurement redundancy of 1.96. The proposed approach yields notably tighter solution hulls for the state variables than both the NP and KO methods, closely approximating the MCS benchmark results. Importantly, all true state values lie within the estimated intervals, confirming the reliability of the proposed ISE framework for LV networks. At the same time, it can be observed that nodes located near the residential PV system exhibit larger interval widths, indicating higher levels of uncertainty.

B. Performance of the AOBBT Algorithm

This section evaluates the performance of the proposed AOBBT algorithm with respect to bound filtering efficiency and computational time under different step sizes.

1) Filtering bounds: Fig. 2 illustrates the evolution of the number of filtered bounds during convergence for two LV networks. It can be observed that smaller step sizes lead to more bounds being filtered at each iteration, while convergence is achieved within approximately 6–8 iterations for all cases. In contrast, the OBBT algorithm requires more than 10 iterations to converge. This behavior occurs because smaller step sizes enable more frequent updates of variable bounds, allowing subsequent micro-rounds of LPs to exploit the progressively tightened bounds and thereby accelerate convergence.

2) Computational Time: The computational times of different ISE methods are summarized in Table II. Across all test cases, the AOBBT algorithm under different step sizes demonstrates substantially improved efficiency compared with the classical OBBT algorithm. Specifically, AOBBT achieves an average speed-up of 194% in the 121-node network and 277% faster in the 321-node network, with similar performance across different step sizes. Considering that smart meter data are typically updated in the scale of several minutes, the proposed approach is suitable for real-time or online applications in LV network monitoring.

TABLE II
COMPUTATION TIME OF DIFFERENT METHODS

Methods	Time (s)	
	121-node	321-node
NP	274.5	1298
KO	164.3	985.4
MCS	2389	6380
Proposed (OBBT)	175.9	2088
Proposed (AOBBT, s=16)	90.8	759.4
Proposed (AOBBT, s=64)	88.1	748.3
Proposed (AOBBT, s=128)	90.5	753.8
Proposed (AOBBT, s=256)	92.4	756.3

VI. CONCLUSIONS

This paper proposes three accelerated strategies for the OBBT algorithm applied to the McCormick relaxation of the ISE problem for LV networks. The proposed Accelerated OBBT algorithm achieves near-global-optimal solutions while significantly reducing the computational burden of conventional OBBT. Numerical validation results demonstrate that the estimation accuracy of AOBBT under different step sizes is comparable to that of the classical OBBT while achieving an average speed-up of of 194% and 277% faster for two LV benchmark networks.

Future research will focus on extending the proposed framework to other strong relaxation techniques to further alleviate bound-tightening stagnation in larger-scale systems.

REFERENCES

[1] A. Bragantini, et al., "Neural network-based three-phase state estimation for unobservable low voltage grids," *Int. J. Elect. Power Energy Syst.*, vol. 167, pp. 1-13, 2025.

[2] B. Liu, et al., "An interval-probability based distribution system state estimation quantification framework considering nonlinear correlations of uncertain distributed generators with limited information," *IEEE Trans. Power Syst.*, vol. 40, no. 3, pp. 2349–2362, May 2025

[3] J. M. Cano et al., "Improving distribution system state estimation with synthetic measurements," *Int. J. Elect. Power Energy Syst.*, vol. 129, pp. 1–6, 2021.

[4] Y. Zhang, et al., "Interval state estimation with uncertainty of distributed generation and line parameters in unbalanced distribution systems," *IEEE Trans. Power Syst.*, vol. 35, no. 1, pp. 762–772, Jan. 2020.

[5] N. VietCuong, W. Wu, and Y. Lou, "Revised constraint-propagation method for distribution interval state estimation." *IET Gener. Transm. Distrib.*, vol. 14, no. 7, pp. 1329-1336, 2020.

[6] N. VietCuong and W. Wu, "Linear programming contractor for interval distribution state estimation using RDM arithmetic," *IEEE Trans. Power Syst.*, vol. 36, no. 3, pp. 2114-2126, 2020.

[7] J. Xu, et al., "An interval arithmetic-based state estimation framework for power distribution networks," *IEEE Trans. Ind. Electron.*, vol. 66, no. 11, pp. 8509–8520, Nov. 2019.

[8] M. Huang et al., "Interval state estimation for low-voltage distribution systems based on smart meter data," *IEEE Trans. Instrum. Meas.*, vol. 68, no. 9, pp. 3090-3099, Sept. 2019.

[9] C. Coffrin, H. L. Hijazi, and P. Van Hentenryck, "The qc relaxation: A theoretical and computational study on optimal power flow," *IEEE Trans. Power Syst.*, vol. 31, no. 4, pp. 3008–3018, Jul. 2016.

[10] F. Cengil, et al., "Learning to accelerate tightening of convex relaxations of the AC optimal power flow problem." *Computational Optimization and Applications*, pp. 1-26, Jul. 2025

[11] A. M. Gleixner, et al., "Three enhancements for optimization-based bound tightening," *J. Glob. Optim.*, vol. 67, no. 4, pp. 731–757, 2016.

[12] D. Liang, et al., "A guaranteed two-stage state estimation framework for unbalanced three-phase distribution systems by considering multi-source measurement uncertainty," *2018 IEEE Power & Energy Society General Meeting* (PESGM), Portland, OR, USA, 2018, pp. 1-5.

[13] A. Navarro-Espinosa and L. Ochoa, "Dissemination document "Low voltage networks models and low carbon technology profiles"," *Ph.D. dissertation*, The University of Manchester, vol. 44, Jun. pp. 1–27, 2015.

979-8-3315-8138-1